The $N_f = 2$ chiral phase transition from imaginary chemical potential with Wilson Fermions

Christopher Pinke[*], **Owe Philipsen**

Institut für Theoretische Physik - Johann Wolfgang Goethe-Universität
Max-von-Laue-Str. 1, 60438 Frankfurt am Main
E-mail: `pinke, philipsen @th.physik.uni-frankfurt.de`

The order of the thermal transition in the chiral limit of QCD with two dynamical flavours of quarks is a long-standing issue. Still, it is not definitely known if the transition is of first or second order. Which of the two scenarios is realized has important implications for the physical QCD phase diagram, and in particular it is important regarding the existence of a critical endpoint at finite densities. Settling this issue by simulating at successively decreased pion mass was not conclusive yet. Recently, an alternative approach was proposed, which relies on the nontrivial phase structure of QCD at purely imaginary chemical potential induced by the Roberge-Weiss symmetry. Using staggered fermions on $N_t = 4$ lattices, it was found that the transition is of first order in the chiral limit. These findings have to be contrasted with other fermion discretizations. We report on the status of our simulations with Wilson fermions following the same approach.
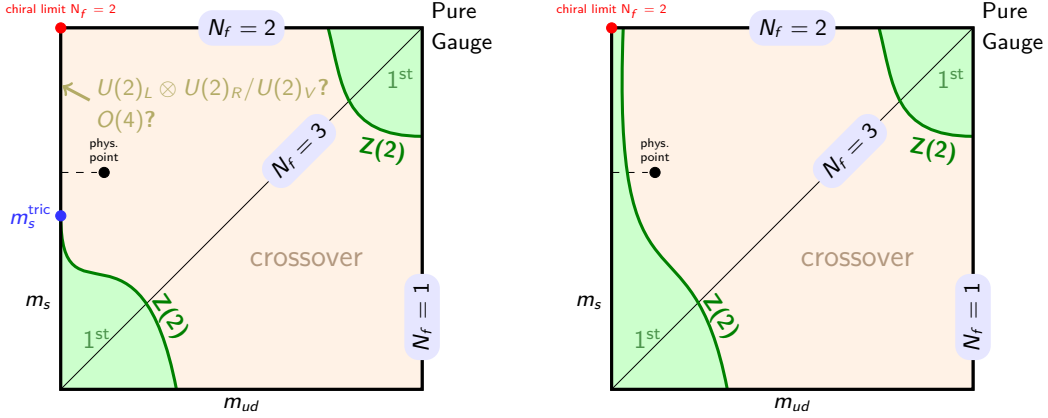
---

[*]Speaker.

Figure 1: *Possible scenarios for the QCD phase diagram at $\mu = 0$ as function of quark mass.*

1. Introduction

The clarification of the order of the thermal transition in the chiral limit of $N_f = 2$ QCD is a long-standing issue. Still, it is not definitely known if the transition is of first or second order. This is depicted in Figure 1. Which of the two scenarios is realized has important implications for the physical QCD phase diagram, and in particular it is important regarding the possible existence of a critical endpoint at finite densities. Settling this issue by simulating at successively decreased pion mass was not conclusive yet, primarily because of the increasing demands of the simulations as the pion mass is lowered (see e.g. [1] for references and a more detailed introduction to the topic).

Recently, an alternative approach was proposed [1], which relies on the nontrivial phase structure of QCD at purely imaginary chemical potential μ_I. In this region of phase space, one has reflection symmetry and extended center (or Roberge-Weiss (RW)) symmetry [4]:

$$Z(\mu) = Z(-\mu), \tag{1.1}$$

$$Z(\mu) = Z(\mu + 2\pi i k / N_c), \, k \in \mathbb{N}. \tag{1.2}$$

These symmetries limit the physically relevant region. Furthermore, at μ_I the sign problem is absent and standard simulation algorithms can be applied. Critical values of $\mu_I^c = (2k+1)\pi / N_c$ ($k \in \mathbb{N}$) mark the boundary between adjacent center sectors. The phase transition between these sectors is first order for high and a crossover for low temperatures. At the endpoint of the first order line, this so-called Roberge-Weiss transition meets with the chiral/deconfinement transition familiar from $\mu = 0$. Consequently, the endpoint is mass-dependent and changes from a triple point at low and high masses to a second order endpoint for intermediate masses. These regions are separated by tricritical points. When mass and N_f are changed, a phase diagram similar to those shown in Figure 1 emerges. Both have to be analytically connected when μ is varied, which is depicted in Figure 2 (left). More specifically, leaving the critical μ_I-values (the bottom of the figure), lines of second order transitions depart from the tricritical points, separating regions of first order transitions from crossover regions. In the vicinity of the tricritical points, the line is governed by tricritical scaling laws, which allows for an extrapolation to the chiral limit. For the $N_f = 2$ backplane, which is of interest in this study, the possible scenarios are shown in Figure 2 (right). If the
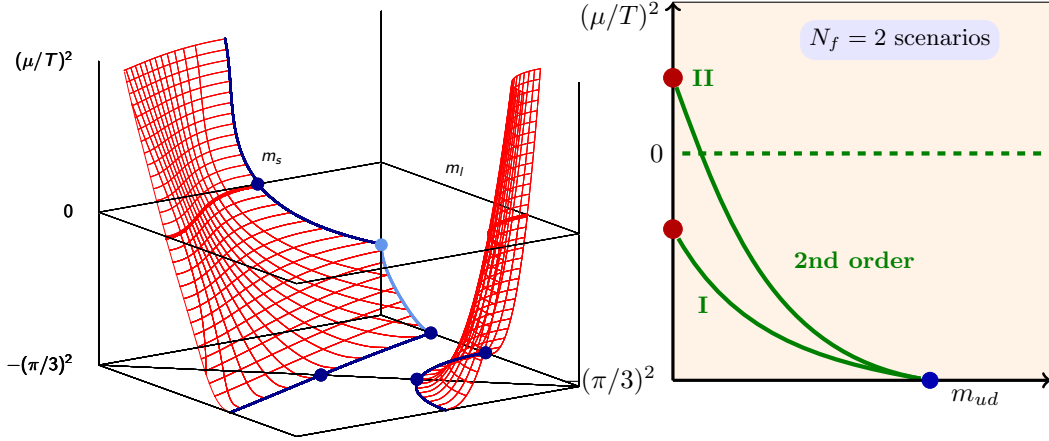
Figure 2: *Left: Expected QCD phase diagram as function of $(\mu/T)^2$. Right: Possible scenarios in the $N_f = 2$ backplane. Both figures follow [1].*

tricritical point at $m = 0$ is at negative values of μ^2, the chiral phase transition is second order. On the other hand, if it is at positive values, there exists a first order region at $\mu = 0$ and the transition in the chiral limit must be first order, too. In this way one can clarify the order of the chiral limit at zero chemical potential by mapping out the second order line. Using staggered fermions on $N_t = 4$ lattices, it was indeed found that the transition is of first order in the chiral limit [1]. These findings have to be contrasted with other fermion discretizations. We report on the status of our simulations with Wilson fermions following the same approach.

2. Simulation details

We employ the same numerical setup as for the previous study described in [2]. That is, in the gauge sector one has the standard Wilson gauge action. In the fermionic sector we consider two flavours of mass-degenerate pure Wilson fermions. The bare fermion mass m is encapsulated in the hopping parameter $\kappa = (2(am+4))^{-1}$. Finite temperature on the lattice is given by the inverse temporal extent, $T = 1/(a(\beta)N_\tau)$. All simulations were carried out using the OpenCL[1] based code CL^{2}QCD [3][2], which runs efficiently on Graphic Processing Units (GPUs) on LOEWE-CSC at Goethe-University Frankfurt [5] and on L-CSC at GSI Darmstadt [6]. We work at fixed temporal lattice extent $N_\tau = 4$, leaving the RW-plane $\mu_I^c = \pi T$ investigated in [2]. In the latter study, the lowest mass simulated was at $\kappa = 0.165$. Consequently, we initialized this study at the same value of the bare quark mass, adding $\kappa = 0.170, 0.175$ and 0.180. In order to locate the critical chemical potential for each bare quark mass, simulations at various values of the quark chemical potential $a\mu$ were carried out. Note that it is possible to transform results obtained at one specific value of the chemical potential to different center sectors due to the RW symmetry (1.2). For each of these parameter sets, temperature scans were carried out with $\Delta\beta$ at least 0.001 around the critical coupling on three spatial volumes, $N_\sigma = 12, 16$ and 20, corresponding to aspect ratios N_σ/N_τ

---

[1]See www.khronos.org/opencl for more information.

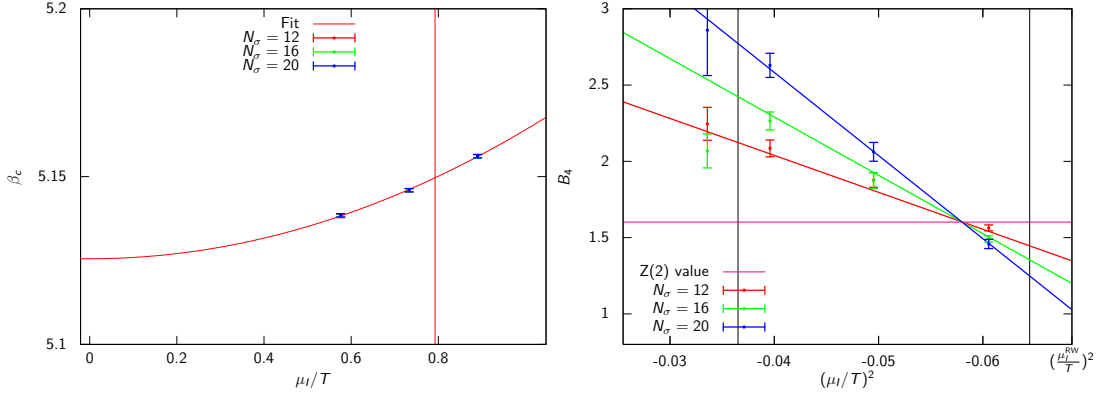[2]Which is now available at github.com/CL2QCD .

Figure 3: *Left: Critical coupling as function of μ/T for $\kappa = 0.170$. The line indicates $\beta_c(\mu_I^c)$. Right: Finite size scaling of B_4 and fit for $\kappa = 0.165$. The vertical lines indicate the fit ranges.*
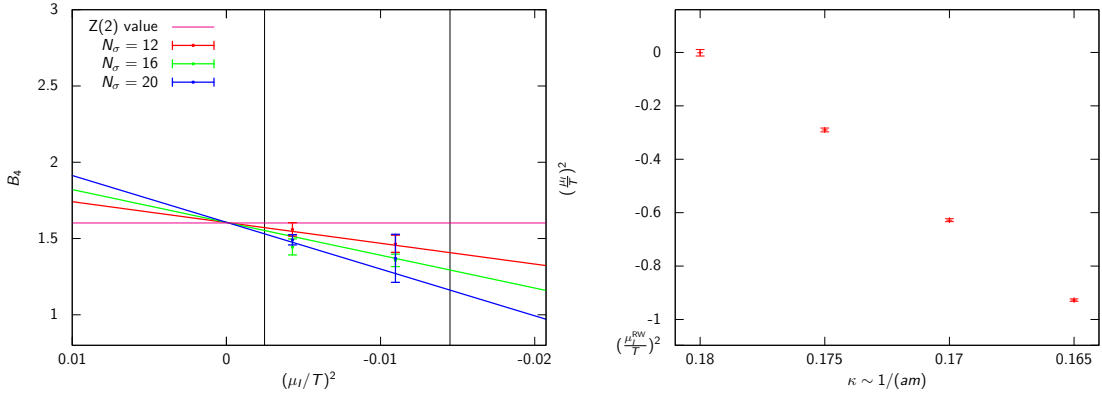

Figure 4: *Left: Preliminary fit results for $\kappa = 0.180$. Right: Results for $\mu_I^c(\kappa)$.*

of 3,4 and 5, respectively. After discarding 5k to 10k trajectories for thermalization, 40k to 60k trajectories have been simulated on each individual Monte-Carlo chain, such that there are at least 100 independent measurements around the critical region. The autocorrelation on the data was estimated using a python implementation[3] of the Wolff method [8]. To accumulate statistics faster, we simulated four chains for each parameter set. Observables are measured after each trajectory and the acceptance rate in each run was of the order of 75%. Additional β-points have been filled in using Ferrenberg-Swendsen reweighting [9].

3. Results

We define a (pseudo-)critical temperature T_c or coupling β_c by the vanishing of the skewness

$$S = \langle (X - \langle X \rangle)^3 \rangle / \langle (X - \langle X \rangle)^2 \rangle^{3/2} \tag{3.1}$$

of a suitable observable X. In this study, we use the chiral condensate $\langle \bar{\psi}\psi \rangle = N_f \, \text{Tr} D^{-1}$. Figure 3 (left) shows β_c for $\kappa = 0.170$ as well as a fit to the data. For a fixed κ, the $\beta_c(\mu)$ can be nicely

---

[3]See github.com/dhesse/py-uwerr .

κ	β_c	$a\mu_I^c$
0.165	5.2421(1)	0.2408(6)
0.170	5.1497(9)	0.1981(9)
0.175	5.0519(3)	0.1346(17)
0.180	4.9520(2)	0.0090(423)

Table 1: *Results for β_c and $a\mu_I^c$ from finite size scaling.*

κ	β	a[fm]	T [MeV]	m_π [MeV]
0.1800	4.9519	0.309(3)	162(2)	587(6)
0.1750	5.0519	0.301(3)	166(2)	642(7)
0.1700	5.1500	0.288(3)	174(2)	699(7)
0.1650	5.2420	0.271(3)	185(2)	770(8)
0.1575	5.3550	0.246(3)	203(2)	929(10)

Table 2: *Results of the scale setting. See text for details.*

fitted to a quadratic, even function, as shown in the figure. This allows to interpolate between simulation points and to extrapolate towards zero chemical potential. As expected, the results show a decreasing critical temperature as the chemical potential approaches zero. The same holds if the (bare) mass is lowered.

In the thermodynamic limit $V \rightarrow \infty$, the Binder cumulant [10]

$$B_4(X) = \langle (X - \langle X \rangle)^4 \rangle / \langle (X - \langle X \rangle)^2 \rangle^2 \tag{3.2}$$

allows to extract the order of the transition. In particular, it takes the values 1 for a first order transition and 3 when there is no true phase transition but a crossover. For the case of a second order transtion in the 3D Ising universality class it has a value of around 1.604 (see e.g. [7]). Hence, a discontinuity exists when passing from the first order to the crossover region via the second order endpoint. To clarify the type of transition on finite lattices one can look at the finite-size scaling of the B_4 at β_c. In the vicinity of the second order point it scales as [10]

$$B_4(\beta_c, N_\sigma) = b_1 + b_2 \left[(a\mu_I)^2 - (a\mu_I^c)^2 \right] N_\sigma^{1/\nu} + \dots . \tag{3.3}$$

For the 3D Ising universality class, one has $b_1 \approx 1.604$ and $\nu \approx 0.63$. The critical coupling μ_I^c indicates the position of the $Z(2)$ endpoint.

The values for $B_4(\beta_c, N_\sigma)$ obtained from the simulations can be fitted to this form. Examples are given in Figure 3 (right) and 4 (left). The results for μ_I^c are shown in Figure 4 (right). Results for β_c and μ_I^c are summarized in Table 1. As can be seen in the figures, B_4 increases with volume if the transition is a crossover (left of the second order point), whereas it decreases in the first order region, ultimately approaching the infinite volume values 3 and 1, respectively. As the (bare) quark mass is lowered, μ_I^c/T decreases towards zero (see Figure 4 (right)). Note that the results for $\kappa = 0.180$ are preliminary. With the given data, one has to extrapolate to μ_I^c (see Figure 4 (left)). Therefore we are currently adding more simulations here in order to get a better estimate of μ_I^c. Nevertheless, μ_I^c is clearly compatible with zero within errors given the current data. This indicates that also for $\mu = 0$ a first order region is present.

To relate these findings to physical scales we performed a series of $T = 0$ simulations at or close to the respective β_c for each κ. Similar to [2] we generated $\mathcal{O}(400)$ independent configurations on $32^3 \times 12$ lattices. With these at hand, we set the scale by the w_0 parameter using the publicly available code described in [11]. This method is based on the Wilson-flow and is very efficient and fast. In particular, it is much more precise than setting the scale by the ρ mass, which was done in [2]. Hence, we revaluated the $T = 0$ simulations from this study, carried out at $\kappa = 0.1575$,
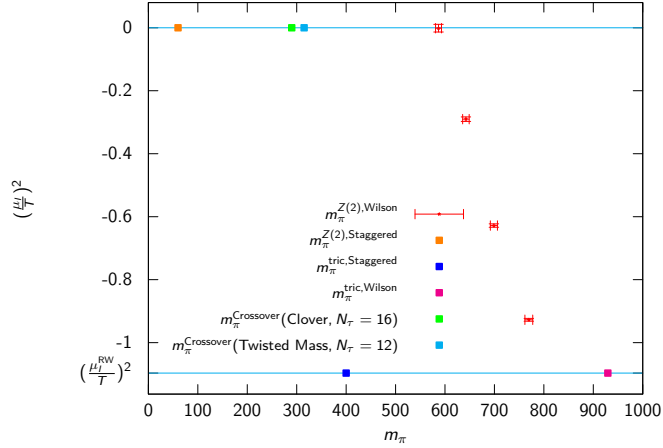
Figure 5: $Z(2)$ *line in the* m_π-$(\mu/T)^2$ *plane. See text for details.*

and include them here for completeness. In addition, the pion mass m_π was determined[4]. The results for the lattice spacing a, the critical temperature T_c and m_π in physical units are summarized in Table 2. The results show that, in terms of pion masses, the first order region is large. Note that the lattices coarsen going to lower masses, since β_c decreases. However, all lattices considered are very coarse, $a \gtrsim 0.25$ fm. Because of this, huge discretization artifacts can be expected. Note that $m_\pi L > 5$ holds for all our parameter sets, so that finite size effects are negligible.

4. Discussion & Perspectives

Our findings are summarized in Figure 5, which shows the $Z(2)$ line in the m_π-μ^2 plane. Leaving the RW-plane, the critical line approaches zero μ at clearly non-vanishing pion masses. In fact, the lowering of the critical pion masses is steady and relatively mild. This finding corresponds to the second scenario sketched in Figure 2 (right).

For comparison, the results from the original study using staggered fermions [1] are also shown in Figure 5. On coarse lattices, both staggered and Wilson discretizations show similar behaviour with a first order region at $\mu = 0$. This region is much larger for Wilson fermions. In ($\mathcal{O}(a)$-improved) Wilson studies at $N_\tau = 12$ [12] and 16 [13], also shown in the figure, only crossover signals are seen, yielding an upper bound for a possible first order region. This suggest that the observed large first order region is to a large extent due to discretization effects.

To put our $N_\tau = 4$ results into perspective, a recent study with $\mathcal{O}(a)$-improved Wilson-Clover fermions determined a similarly large m_π^c of around 880 MeV for $N_f = 3$ on $N_\tau = 4$ lattices[14]. This may suggest that the $\mathcal{O}(a)$ effects are not dominant, at least not on $N_\tau = 4$ lattices.

To reduce cut-off effects, one has to study the N_τ-dependence of the first order region. In another study presented at this conference [15], it was shown that the tricritical point in the RW-plane moves to lower masses by roughly 100 MeV within our setup. We will determine this dependence for the $\mu = 0$ endpoint of the chiral critical line in future studies.

---

[4]We thank F. Depta for carrying out these measurements.

Acknowledgments

O. P. and C. P. are supported by the Helmholtz International Center for FAIR within the LOEWE program of the State of Hesse. C.P. thanks the staff of LOEWE-CSC and L-CSC for their support.

References

[1] C. Bonati, P. de Forcrand, M. D'Elia, O. Philipsen and F. Sanfilippo, Phys. Rev. D **90** (2014) 7, 074030 [arXiv:1408.5086 [hep-lat]].

[2] O. Philipsen and C. Pinke, Phys. Rev. D **89** (2014) 9, 094504 [arXiv:1402.0838 [hep-lat]].

[3] M. Bach, V. Lindenstruth, O. Philipsen and C. Pinke, Comput. Phys. Commun. **184** (2013) 2042 [arXiv:1209.5942 [hep-lat]].

[4] A. Roberge and N. Weiss, Nucl. Phys. B **275** (1986) 734.

[5] M. Bach *et al.*, Computer Science - Research and Development **26** (2011)

[6] D. Rohr, M. Bach, G. Neskovic, V. Lindenstruth, C. Pinke and O. Philipsen, High Performance Computing LNCS **9137** (2015)

[7] H. Blöte *et al.*, J. Phys. A: Math. Gen. **28** (1995)

[8] U. Wolff [ALPHA Collaboration], Comput. Phys. Commun. **156** (2004) 143 [Comput. Phys. Commun. **176** (2007) 383] [hep-lat/0306017].

[9] A. M. Ferrenberg and R. H. Swendsen, Phys. Rev. Lett. **63** (1989) 1195.

[10] K. Binder, Z. Phys. B **43** (1981) 119.

[11] S. Borsanyi *et al.*, JHEP **1209** (2012) 010 [arXiv:1203.4469 [hep-lat]].

[12] F. Burger *et al.* [tmfT Collaboration], Phys. Rev. D **87** (2013) 7, 074508 [arXiv:1102.4530 [hep-lat]].

[13] B. B. Brandt *et al.*, PoS LATTICE **2014** (2015) 234 [arXiv:1410.5981 [hep-lat]].

[14] A. Ukawa *et al.*, Phys. Rev. D **91** (2015) 1, 014508 [arXiv:1411.7461 [hep-lat]].

[15] C. Czaban, F. Cuteri, O. Philipsen, C. Pinke, A. Sciarra, PoS LATTICE **2015** (2015) 148